Macromolecules
ARTICLE

Macromolecules **2010**, *43*, 10031–10037 **10031**
DOI: 10.1021/ma102168a

Temperature Induced Structure Evolution of Regioregular Poly(3-hexylthiophene) in Dilute Solution and its Influence on Thin Film Morphology

Ye Huang, He Cheng,* and Charles C. Han*

State Key Laboratory of Polymer Physics and Chemistry, Joint Laboratory of Polymer Science and Materials, Beijing National Laboratory for Molecular Sciences, Institute of Chemistry, CAS, Beijing 100080, P. R. China

Received September 18, 2010; Revised Manuscript Received October 24, 2010

ABSTRACT: The structure evolution of regioregular poly(3-hexylthiophene) (P3HT) in THF dilute solution and its influence on thin film morphology were studied by a combination of static and dynamic laser light scattering (SLS and DLS) and transmission electron microscopy (TEM). Most P3HT is not directly soluble in THF at room temperature. A thermal treatment at high temperature effectively redisperses P3HT microsized aggregates, and introduces two modes in DLS measurement. The fast mode with $\langle R_h \rangle_f \sim 4$ nm is P3HT unimer coil, while the slow mode with $\langle R_h \rangle_s \sim 90$ nm is P3HT associate. The linear relationship between $\langle \Gamma \rangle$ and q^2 passing through origin indicated both modes are diffusive. DLS showed the percentage of large associates is increasing, and that of the unimer coils is decreasing with temperature. The ratio, $\langle R_g \rangle_s / \langle R_h \rangle_s \sim 0.8$, indicates the associates are closely packed spherical in shape. The structure of P3HT in dilute solution greatly influences its morphology on thin films. We found that the memory of chain conformation and association in solution are carried into drop casted film, TEM examination of drop casted thin film morphology clearly indicated that the densely packed spherical associates are elastic with its morphology unchanged during evaporation process because of its visco-elastic nature; while the P3HT unimer coils assemble and crystallize into nanofibrils. The nanofibrils' percentage decreases with temperature because the coexistence equilibrium between P3HT unimer and spherical associates shifts greatly to the associates side. However, this apparent equilibrium of unimer−associate is in a metastable state. Over a long time, the system will gradually form larger and more stable aggregates which are in equilibrium with unimers at room temperature. Overall, after a proper thermal treatment in solution, it suppresses aggregates formation and increases electronic and opto-physics properties when drop casting is conducted at room temperature.

Introduction

As a novel semiconducting and nonlinear optical material, π-conjugated polymer has drawn a great deal of attention for decades.[1] Its electro- and opto-physical properties are controlled by their chain conformation and assembled structure. However, detailed report on the structural information about most π-conjugated polymer is quite rare.[2−4] It may be partly attributed to the fact that the first generation of this polymer is insoluble and unstable.

With the development of modern synthesis techniques, it was found that a proper modification of polythiophene's rigid backbone makes it soluble, meltable, while keeps its conductivity. However, it is still debatable and not clear whether this modification renders the polymer to be soluble on a molecular level or in an associated structure. In view of this, various nondestructive methods, such as laser light scattering (LS),[2] small-angle X-ray scattering (SAXS),[3] and small angle neutron scattering (SANS)[4] are involved in solving this problem. Most studies indicated that conjugated polymers undergo interchain aggregation easily in the solution state, even under high dilution.[5−8] However, Pearson et al.[2] used a combination of static and dynamic laser light scattering to study the structure of P3HT synthesized via oxidation polymerization (low regularity) in dilute THF solution, and concluded that THF is a moderately good solvent and P3HT macromolecules exist as isolated flexible-coil chains with the persistence length of 2.4 ± 0.3 nm. Aime et al.[4] studied the structure of poly(3-butylthiophene) (P3BT) (low regularity, too) in deuterated nitrobenzene by SANS. Although he claimed that P3BT is isolated neutral chain with flexible coil conformation at 65 °C, the clear low-q upturn indicates interchain association still exists. Chen et al.[9] studied the structure of poly(2,3-diphenyl-5-decyl-1,4-phenylenevinylene) (DP 10-PPV) in THF and toluene by SANS and LS. They concluded that this DP 10-PPV is a more extended worm like chain in chloroform. However, the same problem arises, that is the low-q upturn, instead of a leveling-off scattering intensity in the Guinier region, seems to indicate that wormlike chain model oversimplified the question.

Recent development of conjugated polymer synthesis method makes this debate more ambiguous. The organometallic polycondensation method enables us to obtain high specificity of head-to-tail configuration of the repeat unites (>93% H−T addition).[10] This improvement of regularity of the head-to-tail addition can sufficiently increase $\pi-\pi$ stacking in the solid state and enhance electronic conduction. However, the addition of $\pi-\pi$ stacking complicates the former debate, i.e. the increase of backbone rigidity and regularity seems to have negative effect on polymer solubility. Berry et al.[11] employed various LS techniques to characterize intermolecular association of regioregular poly(3-decylthiophene) P3DT as a function of the thermal history in chloroform. He proposed that under some conditions, the aggregated moiety appears to have a disk-like shape at room temperature. While under other

*Corresponding authors: E-mail: (C.C.H.) c.c.han@iccas.ac.cn; (H.C.) chenghe@iccas.ac.cn. Telephone: +86-10-8261-8089. Fax: +86-10-6252-1519.

Published on Web 11/10/2010

conditions, elongated supermolecular structures are formed with the polythiophene chains in an extended structure especially at low temperature. While Yamamoto et al.[10] used viscometric and light scattering analyses to study poly(3-alkylthiophene-2, 5-diyl)s $CHCl_3$ solutions, and concluded that regioregular P3HT is just more linear and rigid than the one with low regularity.

In this manuscript, we used regioregular P3HT in THF as a model system, and the combination of DLS, SLS, and TEM as the main tools to study solution stability and structural questions. DLS and SLS give us a real-time reciprocal space measure of the P3HT structural variation in solution, and polymer structures in solution can be connected with its morphology in the bulk state measured by TEM. Our results indicated that P3HT structure in solution strongly influence its thin film morphology. And P3HT solution behavior is controlled by polydispersity of molecule weight (M_w) and visco-elastic effect.[12] Therefore, a proper control of its solution structure could greatly enhance its thin film electronic properties.

Experimental Section

Materials and Methods. P3HT was synthesized using a nickel compound as the catalyst according to literature.[13] In order to obtain the so-called narrow-dispersed, well-defined samples, P3HT was fractionated by Soxhlet extraction using a sequence of four solvents including: methanol, *n*-hexane, CH_2Cl_2, and THF. All of the resultant fractions had been dried in vacuum oven for 3 days at 60 °C. The sample with apparent $M_n = 1.6 \times 10^4$ g/mol and $M_w/M_n = 1.5$, was used in the present study. (The sample was thermal-treated to transparent solution and then filtered before GPC measurement which was conducted at 35 °C with THF as eluant and polystyrene as standard.) Reagent grade tetrahydrofuran (THF) was used in LS, which was bought from Sinopharm Chemical Reagent Beijing Co., Ltd., used as received. The solution concentration in LS measurement was fixed at 1 mg/mL. After thermal treatment at 55 °C for 20 min, solutions were filtrated with 0.22 μm Millipore filters at about 20 °C immediately.

Light Scattering (LS) Measurements. A commercial LS spectrometer equipped with a multi-τ digital time correlator (ALV5000) and a cylindrical 22 mW UNIPHASE He−Ne laser (λ_o = 632.8 nm) was used. The spectrometer has a high coherence factor of $\beta \sim 0.95$ because of a novel single-mode fiber optical coupled with an efficient avalanche photodiode as the detector. The LS cell is held in a thermostat refractive index matching vat filled with purified and dust-free toluene, with the temperature controlled within ±0.1 °C. In static LS, the angular dependence (15−150°) of the excess absolute time-averaged scattered intensity, i.e., the Rayleigh ratio $R_{vv}(q)$, which leads to the weight-averaged molar mass M_w and the z-averaged root-mean-square radius of gyration $\langle R_g^2 \rangle_z^{1/2}$ (or written as $\langle R_g \rangle$) of scattering objects,[14] where q is the scattering vector. In dynamic LS (DLS), the intensity−intensity time correlation function $g^{(2)}(t,q)$ in the self-beating mode was measured, where t is the decay time. $g^{(2)}(t,q)$ can be related to the normalized first-order electric field time correlation function $|g^{(1)}(t,q)|$ via the Siegert relation as $g^{(2)}(t,q) = A[1 + \beta|g^{(1)}(t,q)|^2]$, where A ($\equiv\langle I(0)\rangle^2$) is the measured baseline. For the broadly distributed relaxation spectrum, $|g^{(1)}(t,q)|$ is related to a characteristic relaxation time distribution $G(\tau)$, $|g^{(1)}(t,q)| \equiv \langle E(0,q)E^*(t,q)\rangle / \langle E(0,q)E^*(0,q)\rangle = \int_0^\infty G(\tau)e^{-t/\tau} d\tau$, as $G(\tau)$ can be calculated from the Laplace inversion of the measured $g^{(2)}(t,q)$.[15] When two diffusive modes were detected, they can be simply characterized by diffusion coefficients D_f, D_s, and the amplitudes A_f, A_s (subscripts f and s refer to faster and slower, respectively). A_f, A_s were evaluated through the moments of distribution functions of decay times $G(\tau)$ obtained by fitting correlation curves using CONTIN programs mentioned above. For a pure diffusive relaxation, Γ can be related to the translational diffusion coefficient D by $(\Gamma/q^2)_{q\to 0, C\to 0} = D$ or a hydrodynamic radius $R_h = k_B T/6\pi\eta D$ with k_B, T, and η being the Boltzmann constant, the absolute temperature and the solvent viscosity, respectively.[15,16] The details of the LS instrumentation and theory can be found elsewhere.[17,18]

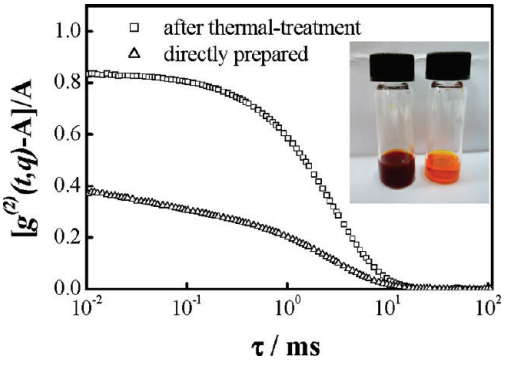

Figure 1. Intensity−intensity time correlation function $[g^{(2)}(t,q) - A]/A$ of P3HT in THF solution. (c = 1 mg/mL, θ = 20°, T = 20 °C): filtered directly (Δ); filtered after the solution was thermal treated (□). The inset shows the contrast photos of P3HT in THF: directly dissolved (left) and after thermal treatment (right).

d*n*/d*c* Measurements. The specific refractive index increment (dn/dc) of the Poly(3-hexylthiophene) in THF after thermal treatment was measured by using a high-precision differential refractometer.[15] At 25 °C, the dn/dc of P3HT in THF was 0.31 mL/g, which is close to 0.3 reported before.[2]

Wide-Angle X-ray Scattering. Wide angle X-ray scattering (WAXS) studies were performed to address the structural properties of P3HT in solutions (10 mg/mL). The WAXS measurements were carried out at room temperature by Rigaku S/Max 1000 Laboratory small angle X-ray scattering with IP (image plate) on MicroMax-007HF generator operated at 40 kV and 30 mA. The wavelength is 1.54 Å. An O-ring and berillium (Be) windows sealed liquid cell was used for the P3HT solution measurements. Solution samples and pure THF are placed in the X-ray beam path and scattered photons were recorded with exposure time of 7200 s. The 2D pattern was calibrated by silica powder and transferred to 1D curve by radial average.

Transmission Electron Microscopy. Transmission electron microscopy (TEM) was performed using a JEOL 2200FS instrument at 160 kV accelerating voltage. For TEM examination, the P3HT solution was diluted to 0.02 mg/mL and then dropped on the copper grid which is covered by carbon membrane. Subsequently, the TEM grid was placed in the vacuum oven for 12 h to remove the solvent.

Results and Discussion

1. LS Determination of P3HT Structure in Dilute Solution. *1.1. Filtration and Heating Influences on P3HT Structure in Dilute THF Solution.* Figure 1 shows that thermal treatment has large influence on the structure of P3HT in solution. The inserted picture shows that the original P3HT THF solution is dark purple and looks turbid if the P3HT was directly dissolved at room temperature (RT). But it is orange in color and transparent if we heat it to 55 °C and then cool it back to RT. After filtration by 0.22 μm filter, the directly dissolved sample leaves most part of P3HT aggregates on the filter membrane, while thermal-treated one does not. The average scattered light intensity increases more than 1200 times after thermal treatment and filtration. All of these indicate that direct dissolution of P3HT in THF at RT is not sufficient to disperse a large portion of aggregates with micro or larger sizes into small scaled structure but thermal treatment can improve this dispersion process. Note that the transparent P3HT THF solution after thermal treatment will go back to dark purple color after 9 days at RT, indicating

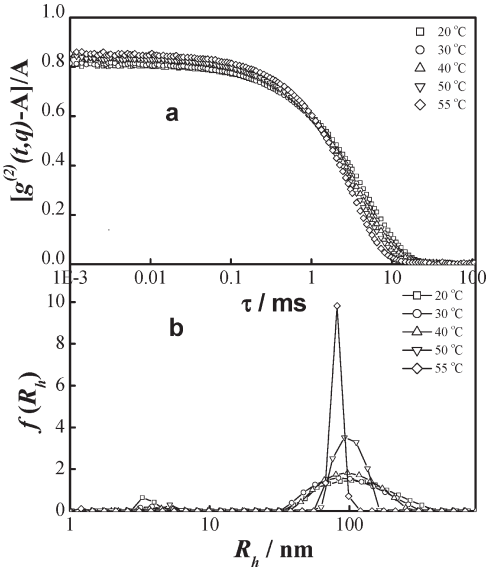

Figure 2. Temperature dependence of autocorrelation function $[g^{(2)}(t,q)$ - A]/A and the corresponding hydrodynamic radius distributions $f(R_h)$ (θ = 20°).

the RT solution after thermal treatment is a metastable or unstable state, and there is strong structure hysteresis in the heating−cooling process which may be originated from polydispersity and visco-elastic effect.[19,20] There are three kinds of particles in the system, the smallest primary particle ($\langle R_h \rangle \sim 4$ nm) is unimer, the intermediate particle ($\langle R_h \rangle \sim 90$ nm) is named as associates, while the largest particle ($\langle R_h \rangle \sim 1$ μm) is denoted as aggregates, respectively. The high temperature (55 °C) can disperse most of the aggregates into associates and unimers.

1.2. DLS Measurement of P3HT Structure in THF Dilute Solution. The structure of P3HT in dilute THF solution can be measured by DLS. After the thermal treatment, the solution is cooled down to RT and filtered. Figure 2a shows the temperature dependent autocorrelation functions after filtration, and Figure 2b gives the corresponding hydrodynamic radius distribution. Two modes appear at all the tested temperatures. The fast mode with a dimension of ~4 nm can be attributed to P3HT unimer coil. Aime concluded that the P3BT in nitrobenzene at 65 °C is a fairly flexible coil, and its statistical length should be comparable to the corresponding value for a typical flexible polymer.[4] Burchsard studied hydrodynamic and thermodynamic behavior of short-chain polystyrene in toluene and cyclohexane at 34.5 °C, and obtained a scaling law between hydrodynamic radius and its molecular weight.[21] According to his calculation, if the fast mode really represented P3HT unimer coil in moderate good solvent,[2] and its persistence length is similar to that of PS in theta solvent, then its hydrodynamic radius should also be about 3.6 nm. It is quite similar to our DLS measurements, the slight difference can be attributed to the P3HT's more rigid backbone. The slow mode with a dimension of ~90 nm is P3HT associates because the $\pi-\pi$ stacking between semirigid chain segments facilitates interchain assemblies. The percentage and distribution of P3HT associates change with temperature. Note that $f(R_h)$ is z-averaged and the scattered light intensity is proportional to the number of solutes and the square of their molecular weight (M_w).[12] Assuming that the associates and unimers have the same scattered density and the scattered intensity is proportional to the square of the M_w since the average size of the associates is about 20 times larger than unimer coils, so the

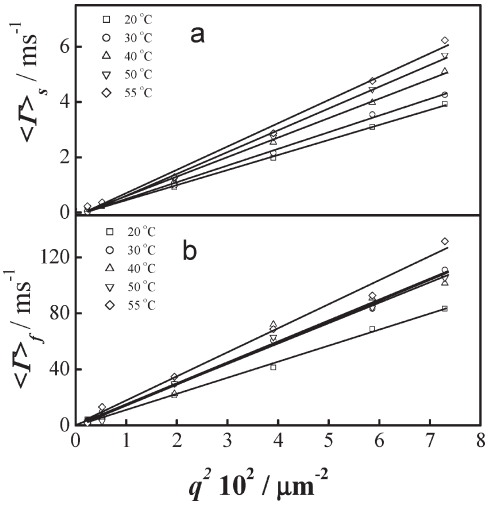

Figure 3. Temperature dependence of $\langle\Gamma\rangle$ vs q^2 in dilute P3HT solution; (a) the slow relaxation (b) the fast relaxation mode. (c = 1 mg/mL).

number of unimer coils should be 6.4×10^7 times that of associates if they contribute the same to the scattered light intensity.[22] In our case, the contribution of associates to the scattered light intensity is no more than 99% at the highest measured temperature, so the number of unimer coil is overwhelmingly about 10^5 to 1 over the number of associates in P3HT THF dilute solution.

A temperature dependence of DLS line-width $\langle\Gamma\rangle$ vs q^2 is presented in Figure 3. For purely diffusive relaxation in dilute solution, $\langle\Gamma\rangle$ is linearly dependent on the square of the scattering vector q, passing through the origin. A straight line passing through the origin reveals that both relaxation modes are purely diffusive in the temperature range from 20 to 55 °C. The fast mode is the diffusive motion of P3HT unimer coil, while the slow mode may be attributed to the diffusive motion of certain spherical associates which will be discussed in the next section.

1.3. SLS Determination of the Basic Shape of Slow Mode Object. The structure of the slow mode object can be better viewed from the ratio between $\langle R_g \rangle_s$ and $\langle R_h \rangle_s$. This is because they are related to the segmental distribution in different ways: $\langle R_g \rangle$ is related to the square average of the segmental distribution $\langle r_{ij}^2 \rangle$ and reflects the density distribution in real space, while $\langle R_h \rangle$ is related to the inverse segmental distribution $\langle r_{ij}^{-1} \rangle$ and is the radius of an equivalent nondraining sphere with the same translational diffusion coefficient. For random coil, hyperbranched cluster and uniform sphere, $\langle R_g \rangle / \langle R_h \rangle$ is 1.5−1.8, 1.0−1.2, and ~0.8, respectively.[23] Figure 4 shows the temperature dependence of $\langle R_g \rangle_s$, $\langle R_h \rangle_s$, and $\langle R_g \rangle_s / \langle R_h \rangle_s$ in the heating process. We can find that during the whole heating process, $\langle R_g \rangle_s / \langle R_h \rangle_s$ of the slow mode keeps constant (~0.8). Combined with the result in Figure 3a that the motion of the particle is purely diffusive; we can conclude that the shape of the slow mode objects is close to a uniform sphere. The P3HT sample was synthesized via Grignard Metathesis method. Its original product must be widely distributed with $M_w/M_n > 2$. Although a sequence of Soxhlet extraction has eliminated most low M_w fractions. There must still be a small number of low M_w and almost all the higher M_w specimen left in the final fraction. The narrowly distributed GPC results must have been caused by the fact that the filtration inside the GPC measurement after the injection has taken out most of the aggregates and associates which were more likely formed by high M_w fractions which have longer $\pi-\pi$ conjugated length, tend to

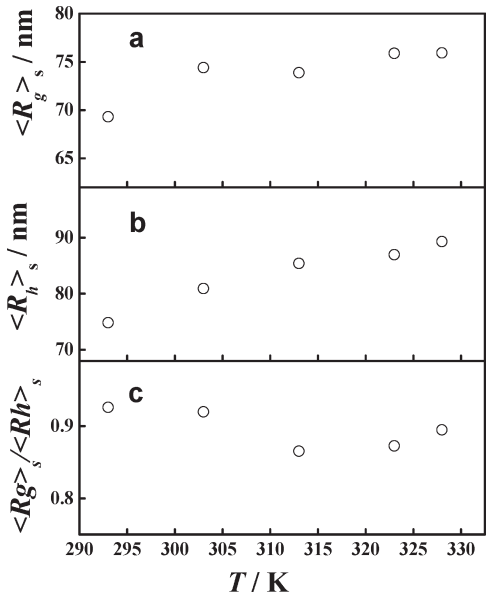

Figure 4. Temperature dependence of (a) the radius of gyration $\langle R_g \rangle_s$, (b) hydrodynamic radius $\langle R_h \rangle_s$ and (c) their ratio $\langle R_g \rangle_s / \langle R_h \rangle_s$ of the slow mode.

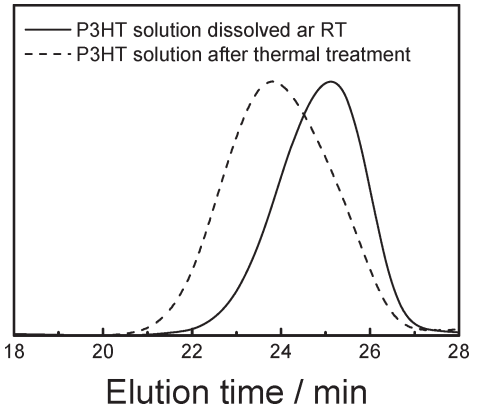

Figure 5. GPC traces of P3HT solution dissolved at RT solution and after thermal treatment. Solvent: THF. Flow rate: 1 mL/min.

form larger aggregates or associates. Recently, it is reported that the formation of P3HT with higher M_w is caused by the difunctional dimers, which was unavoidable in the process of the Grignard metathesis method catalyzed by nickel compound.[24,25] In our case, a thermal treatment at 55 °C destroys and redisperses all those microsized aggregates. The metastable state of the solution is a coexistence of unimer P3HT and a small number of spherical associates which may be formed by high M_w macromolecules to minimize their surface energy. This assumption can be proved by GPC measurement. Figure 5 is the GPC traces of P3HT solution dissolved at RT and after thermal treatment. It clearly demonstrates that the P3HT sample after thermal treatment has a relatively higher M_w and broader distribution than that being directly filtered. In addition, GPC curve of the sample dissolved at RT is not very symmetric which means that there are a small number of low M_w and almost all the high M_w specimen left after soxhlet fractionation. Thermal treatment can effectively dissolve part of relatively high M_w P3HT fraction and redisperse the microsized aggregates. In this report, we shall only deal with the equilibrium between the unimers and the associates prepared through high temperature treatment of original sample in THF. Although this

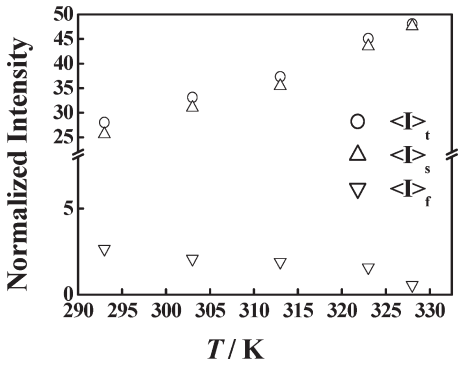

Figure 6. Temperature evolution of the normalized total, slow and fast modes scattered light intensity of the P3HT solution after thermal-treatment and filtration ($\theta = 20°$).

unimer/associate may be a system trapped in a metastable state and could eventually fall into a lower free energy state of aggregate/unimer coexistence state at RT (after 7−9 days). We will discuss that long time aggregate/unimer state in our next report.

1.4. SLS Determination of the P3HT Structure Development in the Heating Process. The total average scattered light intensity ($\langle I \rangle_t$) comes from the summation of contributions from unimer coils $\langle I \rangle_f$ and associates $\langle I \rangle_s$, where the solvent contribution has been substrated, namely, with $\langle I \rangle_t = \langle I \rangle_f + \langle I \rangle_s$ and $\langle I \rangle_f = \langle I \rangle_t A_f$, $\langle I \rangle_s = \langle I \rangle_t A_s$, and $A_f + A_s = 1$, where A_f and A_s are the intensity weight fractions of the fast and slow modes, respectively. The separation of the contribution from fast or slow mode facilitates us to find out the tendency of P3HT unimer-associate distribution with temperature. Figure 6 shows the temperature evolution of the normalized total, slow and fast modes scattered light intensity of the P3HT solution after thermal-treatment and filtration. We can find that both $\langle I \rangle_t$ and $\langle I \rangle_s$ increase with temperature, while the contribution from fast mode scattered light intensity ($\langle I \rangle_f$) decreases. At 55 °C, the $\langle I \rangle_f$ is close to zero. The dynamic equilibrium between unimer coils and associates shifts severely to the associates' side with temperature. More and more unimer coils segregate to associates, so the percentage of the associates is increasing with temperature. All of these phenomena seem to indicate that it is a LCST process for a transition between the unimers and the associates. However, the original P3HT THF solution is full of microsized aggregates and not soluble at all without thermal treatment at higher temperature, which is UCST in nature between the associates and the aggregates. This counterintuitive phenomenon may be originated from the facts that P3HT particles are polydispersed. It has been proved that common GPC results about single P3HT information are not correct, the relatively narrow GPC peak did not mean that the P3HT sample used is narrowly dispersed. In fact, it is rather polydispersed, because the associates are composed mainly of high molecular weighted P3HT fractions which have been filtered out before GPC measurement. Note that different fractions may have the same kind of phase diagram, but different critical points. And this apparent unimer-associate equilibrium is only a metastable equilibrium. In this manuscript, we are focusing on how metastable state formed by the polydisperse P3HT sample influences on its drop-casted film morphology. The kinetics of narrowly distributed P3HT structure variation with temperature and its relationship with aggregates will be discussed in a different manuscript. The coexistence of unimer and associates is

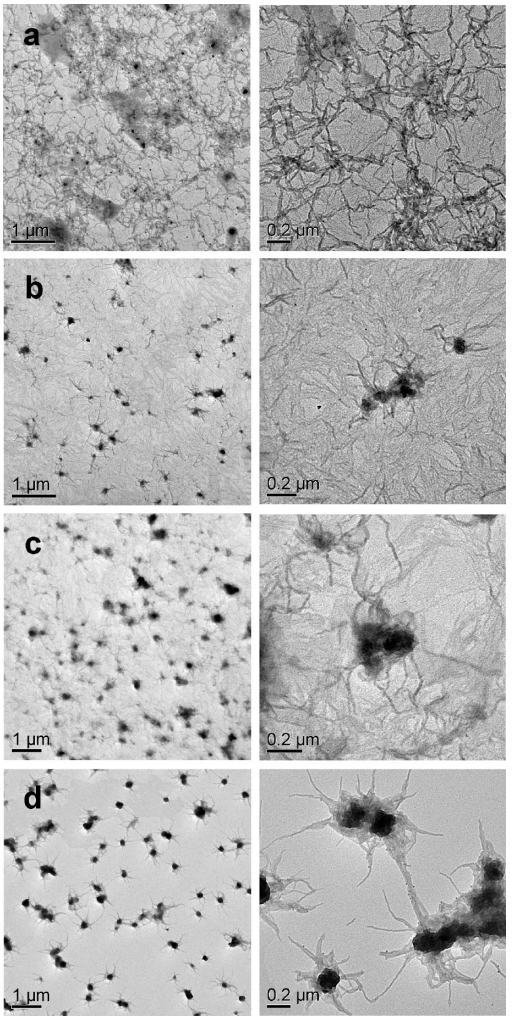

Figure 7. TEM micrographs depicting morphology evolutions of drop-casting P3HT films from studies at different temperatures: (a) 20 °C; (b) 40 °C; (c) 50 °C; (d) 55 °C at two different levels of magnification.

stable at 50 °C; i.e., the scattered light intensity, $\langle R_g \rangle_s$, $\langle R_h \rangle_s$, $\langle R_g \rangle_s / \langle R_h \rangle_s$ can be repeated for 3 days with increasing and decreasing temperatures.

2. TEM Evaluation of P3HT Solution Structure Influence on the Morphology of Casted Films. The memory of chain structure in P3HT solution is carried into drop casting film. Figure 7 is the TEM micrographs of P3HT drop casted film morphology from studies at different temperatures. It clearly indicated that nanofibrils, with average width about 18 ± 4 nm are dominated at low temperature, while P3HT associates with a dimension of ~180 nm are dominated at high temperature. The size of those associates is almost the same as that in solution ($2\langle R_h \rangle \sim 180$ nm) and it looks like dried broken sphere. Specimen casted from 55 °C solution, the nanofibrils are rare. The percentage of the associates is increasing with temperature. So it agrees well with our DLS measurements. The reason that those spherical associates almost did not interpenetrate to form larger aggregates during solvent evaporation can be explained by the viscoelastic effect.

Picarra and Martinho[26] showed that in the phase separation of a thin-layer dilute homopolymer solution on the surface, the collision would not be effective as long as the collision (or contact) time (τ_c) is shorter than the entanglement time (τ_e) needed to establish a permanent chain entanglement between two approaching aggregates. Quantitatively,

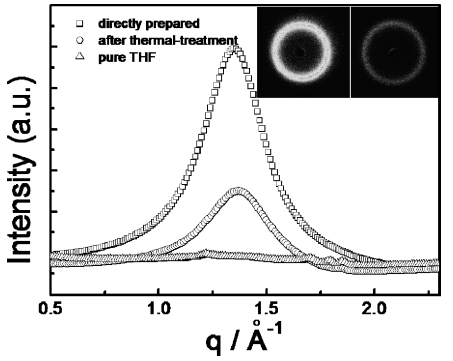

Figure 8. WAXS patterns of P3HT solution dissolved at room temperature, after thermal treatment and pure THF, the insets are the 2D spectra corresponding to P3HT solution room temperature (left), after thermal treatment (right).

Tanaka[19,20] showed that τ_c and τ_e could be roughly characterized as

$$\frac{l_o}{\langle v \rangle} < \tau_c < \frac{{l_o}^2}{\langle D \rangle} \quad \text{and} \quad \tau_e \sim \frac{{a_m}^2 {N_m}^3 {\phi_p}^{3/2}}{D_m} \tag{1}$$

where l_o is the interaction range, $\langle v \rangle$ and $\langle D \rangle$ are the mean thermal velocity and transitional diffusion coefficient of associates, respectively, ϕ_p is the average polymer concentration inside associates, and a_m, N_m and D_m is the length, number and diffusion coefficient of monomer, respectively. When $\tau_c \ll \tau_e$, two colliding associates have no time to stick together and they behave just like two tiny nonadhesive "elastic" balls. Such an effect is a character of the viscoelasticity of long polymer chains. For a given polymer solution under certain experimental conditions, l_o, a_m, N_m, D_m in eq 1 are constants. One can only increase $\langle D \rangle$ and ϕ_p to ensure that $\tau_c \ll \tau_e$ in order to have a stable associates phase. On the one hand, the diffusion coefficient of associates ($\langle D \rangle_s$) increases with temperature, which can reduce τ_c. The strong $\pi-\pi$ stacking between P3HT segments inside associates gives sufficiently high ϕ_p. So the acceleration of the evaporation rate of solvent with temperature during drop-casting process results in higher ϕ_p and τ_e. Correspondingly, it enables P3HT associates to be closely packed into uniform and "elastic" like sphere. Also it will prevent them from interpenetrating with each other in the evaporation and cooling process.

Nanofibrils may be contributed to the self-assembly of P3HT unimer coils during solvent evaporation process. The unimer coil moves much faster and has sufficient time to pack into nanofibrils under evaporation.[27−29] Smith et al.[30] reported that P3ATs may crystallize from dilute solutions in poor solvents (such as cyclohexane) in the form of well-defined, ribbon-like crystals, or whiskers. Bao et al. also claimed that P3HT in THF solution can form short nanofibrils during THF evaporation.[27] They proved that solution concentration can affect the length of the nanofibrils, but the width of them almost stays constant, ~18 nm.[27] An increase of temperature lowers its molar percent in solution, so nanofibrils are rare at 55 °C, as demonstrated in SLS measurements. In the cooling process, the coexistence of spherical associates and unimer coils also need to pass through various metastable states which are induced by P3HT polydispersity to get to the final thermodynamically and kinetically stable, precipitation of aggregates state. On the one hand, the precipitation process is very long around, 9 days at room temperature, which may be caused by the facts that it is not far away from the phase boundary, or the

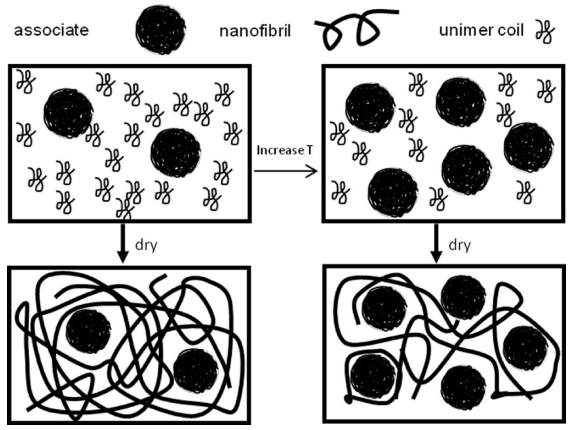

Figure 9. Schematic illustration of P3HT structure in THF dilute solution at 20 and 55 °C after thermal treatment and its corresponding drop casting thin film morphology.

spherical associates are quite elastic and not very easy to interpenetrate with each other. On the other hand, the M_w dependence of the aggregate formation and their equilibrium with associates and unimers will be discussed later in a separate report.

3. WAXS Investigation of the Amorphous Nature of P3HT Associates. Our research result does not support the assumption that the aggregates in the solution is microcrystalline.[31] Figure 8 shows the WAXS patterns of our P3HT solution prepared via two different ways: directly dissolved at RT and after thermal treatment, respectively. The effect of THF has been excluded as pure THF has no WAXS information. No sharp crystalline peaks but a big amorphous halo is observed at 4.6 Å which does not belongs to any characteristic crystalline distance but can be attributed to the distance between centers of thiophene rings because of its larger electron density.[32,33] Neher et al. studied nanocrystal structure of P3HT powder and found that there are several sharp peaks in the WAXS results.[34] However, there is only one big halo but any detailed crystal structure in the solution sample, so we may conclude that the associates are amorphous in nature instead of microcrystallines in THF solution.

The whole process can be illustrated in Figure 9. After thermal treatment, most P3HT is unimer coils in THF aqueous solution. A small portion of them segregates together to form spherical associates. The associates' population increases with temperature, but the size is fixed because of its visco-elastic nature. P3HT structure in solution lasts through evaporation process in the drying process and P3HT associates keep its size and shape, while unimer coils pack into nanofibrils.

Conclusion

P3HT structure in dilute solution and its influences on thin film morphology were studied both in real and reciprocal spaces. DLS showed that there are two modes in P3HT THF solution, the fast mode is P3HT unimer coils, and the slow mode is spherical P3HT associates. However, SLS measurement indicated that the percentage of unimer coils is decreasing but that of associates is increasing with temperature. All of these effects strongly influence the thin film morphology of P3HT, because P3HT unimer-associates distribution sets the initial state of the film morphology formed. Associates keep their size and shape during the drying and initial cooling process because of their visco-elastic nature and increase their population with solution temperature. The nanofibrils in the dry films are originated from the packing of P3HT unimer coils. So, after thermal treatment, drop-casting conducted at lower temperature will enhance electronic and optophysical properties of the final products due to the higher fraction of nanofibrils content

Acknowledgment. The financial support from the National Natural Science Foundation of China (Young Scientists Fund) (20804052) is gratefully acknowledged.

References and Notes

(1) Skotheim, T. A.; Elsenbaumer, R. L.; Reynolds, J. R. *Handbook of Conducting Polymers*, 2nd ed., Dekker: New York, 1998.
(2) Heffner, G. W.; Pearson, D. S. *Macromolecules* **1991**, *24* (23), 6295–6299.
(3) Narsimlu, N.; Kumar, K. S.; Wu, C. E.; Wu, C. G. *Mater. Lett.* **2004**, *58* (6), 1113–1116.
(4) Aime, J. P.; Bargain, F.; Schott, M.; Eckhardt, H.; Miller, G. G.; Elsenbaumer, R. L. *Phys. Rev. Lett.* **1989**, *62* (1), 55–58.
(5) Collison, C. J.; Rothberg, L. J.; Treemaneekarn, V.; Li, Y. *Macromolecules* **2001**, *34* (7), 2346–2352.
(6) Grell, M.; Bradley, D. D. C.; Long, X.; Chamberlain, T.; Inbasekaran, M.; Woo, E. P.; Soliman, M. *Acta Polym.* **1998**, *49* (8), 439–444.
(7) Chen, S. H.; Su, A. C.; Huang, Y. F.; Su, C. H.; Peng, G. Y.; Chen, S. A. *Macromolecules* **2002**, *35* (11), 4229–4232.
(8) Nguyen, T. Q.; Doan, V.; Schwartz, B. J. *J. Chem. Phys.* **1999**, *110* (8), 4068–4078.
(9) Li, Y. C.; Chen, C. Y.; Chang, Y. X.; Chuang, P. Y.; Chen, J. H.; Chen, H. L.; Hsu, C. S.; Ivanov, V. A.; Khalatur, P. G.; Chen, S. A. *Langmuir* **2009**, *25* (8), 4668–4677.
(10) Yamamoto, T.; Oguro, D.; Kubota, K. *Macromolecules* **1996**, *29* (5), 1833–1835.
(11) Yue, S.; Berry, G. C.; McCullough, R. D. *Macromolecules* **1996**, *29* (3), 933–939.
(12) Zhang, G. Z.; Wu, C. *Conform.-Depend. Des. Sequences Copolym. I* **2006**, *195*, 101–176.
(13) Loewe, R. S.; Khersonsky, S. M.; McCullough, R. D. *Adv. Mater.* **1999**, *11* (3), 250–253.
(14) Wang, J.; Wang, Z. L.; Peiffer, D. G.; Shuely, W. J.; Chu, B. *Macromolecules* **1991**, *24* (3), 790–798.
(15) Wu, C.; Xia, K. Q. *Rev. Sci. Instrum.* **1994**, *65* (3), 587–590.
(16) Wu, C.; Zhou, S. Q. *J. Polym. Sci., Part B: Polym. Phys.* **1996**, *34* (9), 1597–1604.
(17) Chu, B. *Laser Light Scattering*; Academic Press: New York, 1974.
(18) Berne, B. J.; Pecora, R. *Dynamic Light Scattering*; Plenum Press: New York, 1976.
(19) Amagishi, Y.; Tanaka, M. *Phys. Rev. Lett.* **1993**, *71* (3), 360–363.
(20) Tanaka, H.; Suzuki, T.; Hayashi, T.; Nishi, T. *Macromolecules* **1992**, *25* (17), 4453–4456.
(21) Huber, K.; Bantle, S.; Lutz, P.; Burchard, W. *Macromolecules* **1985**, *18* (7), 1461–1467.
(22) Here

$$\frac{Kc}{R_\theta} = \frac{1}{M_w}\left(1 + \frac{1}{3}q^2\langle R_g^2\rangle_z + 2A_2M_wc + \ldots\right)$$

when $c \to 0$, $q \to 0$, $I \propto R_\theta \propto cM_w$, c is the mass concentration and M_w is the weight-average molecular weight. As $c \propto nM_w$, $I \propto nM_w^2$. When we assume that $I_f = I_s$, $\rho_f = \rho_s$, and $M = {}^4/_3\pi\rho R^3$

$$\frac{I_f}{I_s} \propto \frac{(nM_w^2)_f}{(nM_w^2)_s} \propto \frac{(nR^6)_f}{(nR^6)_s}$$

we can get n_f/n_s.
(23) Burchard, W., Brown, W., Eds.; Clarendon Press: Oxford, U.K., 1996; p 439.
(24) Iovu, M. C.; Sheina, E. E.; Gil, R. R.; McCullough, R. D. *Macromolecules* **2005**, *38* (21), 8649–8656.
(25) Miyakoshi, R.; Yokoyama, A.; Yokozawa, T. *J. Am. Chem. Soc.* **2005**, *127* (49), 17542–17547.
(26) Picarra, S.; Martinho, J. M. G. *Macromolecules* **2001**, *34* (1), 53–58.
(27) Yang, H. C.; Shin, T. J.; Yang, L.; Cho, K.; Ryu, C. Y.; Bao, Z. N. *Adv. Funct. Mater.* **2005**, *15* (4), 671–676.
(28) Chang, J. F.; Sun, B. Q.; Breiby, D. W.; Nielsen, M. M.; Solling, T. I.; Giles, M.; McCulloch, I.; Sirringhaus, H. *Chem. Mater.* **2004**, *16* (23), 4772–4776.

(29) DeLongchamp, D. M.; Vogel, B. M.; Jung, Y.; Gurau, M. C.; Richter, C. A.; Kirillov, O. A.; Obrzut, J.; Fischer, D. A.; Sambasivan, S.; Richter, L. J.; Lin, E. K. *Chem. Mater*. **2005**, *17* (23), 5610–5612.
(30) Ihn, K. J.; Moulton, J.; Smith, P. *J. Polym. Sci., Part B: Polym. Phys*. **1993**, *31* (6), 735–742.
(31) Rughooputh, S. D. D. V.; Hotta, S.; Heeger, A. J.; Wudl, F. *J. Polym. Sci., Part B: Polym. Phys*. **1987**, *25* (5), 1071–1078.
(32) Kline, R. J.; Mcgehee, M. D.; Toney, M. F. *Nat. Mater*. **2006**, *5* (3), 222–228.
(33) Sirringhaus, H.; Brown, P. J.; Friend, R. H.; Nielsen, M. M.; Bechgaard, K.; Langeveld-Voss, B. M. W.; Spiering, A. J. H.; Janssen, R. A. J.; Meijer, E. W.; Herwig, P.; de Leeuw, D. M. *Nature* **1999**, *401* (6754), 685–688.
(34) Zen, A.; Saphiannikova, M.; Neher, D.; Grenzer, J.; Grigorian, S.; Pietsch, U.; Asawapirom, U.; Janietz, S.; Scherf, U.; Lieberwirth, I.; Wegner, G. *Macromolecules* **2006**, *39* (6), 2162–2171.